JOURNAL OF BACTERIOLOGY, Dec. 2005, p. 7945–7954 Vol. 187, No. 23
0021-9193/05/$08.00+0 doi:10.1128/JB.187.23.7945–7954.2005

Enterobacterial Repetitive Intergenic Consensus Sequence Repeats in Yersiniae: Genomic Organization and Functional Properties

Eliana De Gregorio,[1] Giustina Silvestro,[1] Mauro Petrillo,[2] Maria Stella Carlomagno,[1] and Pier Paolo Di Nocera[1]*

Dipartimento di Biologia e Patologia Cellulare e Molecolare, Facoltà di Medicina, Università Federico II, Via S. Pansini 5, 80131 Napoli, Italy,[1] and CEINGE Biotecnologie Avanzate s.c.a.r.l., Via Comunale Margherita n. 482, 80131 Napoli, Italy[2]

Received 29 July 2005/Accepted 21 September 2005

Genome-wide analyses carried out in silico revealed that the DNA repeats called enterobacterial repetitive intergenic consensus sequences (ERICs), which are present in several *Enterobacteriaceae*, are overrepresented in yersiniae. From the alignment of DNA regions from the wholly sequenced *Yersinia enterocolitica* 8081 and *Yersinia pestis* CO92 strains, we could establish that ERICs are miniature mobile elements whose insertion leads to duplication of the dinucleotide TA. ERICs feature long terminal inverted repeats (TIRs) and can fold as RNA into hairpin structures. The proximity to coding regions suggests that most *Y. enterocolitica* ERICs are cotranscribed with flanking genes. Elements which either overlap or are located next to stop codons are preferentially inserted in the same (or B) orientation. In contrast, ERICs located far apart from open reading frames are inserted in the opposite (or A) orientation. The expression of genes cotranscribed with A- and B-oriented ERICs has been monitored in vivo. In mRNAs spanning B-oriented ERICs, upstream gene transcripts accumulated at lower levels than downstream gene transcripts. This difference was abolished by treating cells with chloramphenicol. We hypothesize that folding of B-oriented elements is impeded by translating ribosomes. Consequently, upstream RNA degradation is triggered by the unmasking of a site for the RNase E located in the right-hand TIR of ERIC. A-oriented ERICs may act in contrast as upstream RNA stabilizers or may have other functions. The hypothesis that ERICs act as regulatory RNA elements is supported by analyses carried out in *Yersinia* strains which either lack ERIC sequences or carry alternatively oriented ERICs at specific loci.

Transposable elements (TEs) are widely distributed in prokaryotic and eukaryotic genomes. TEs are broadly divided into two classes according to their transposition intermediates. Class 1 elements transpose by means of an RNA intermediate and feature either long terminal direct repeats or a poly(A) tract at one end. Class 2 elements transpose by means of a DNA intermediate, and most have terminal inverted repeats (TIRs). Integration of most TEs frequently determines the duplication of target sites of fixed lengths (20).

DNA repeats which recall class 2 elements in terms of the presence of TIRs but have no coding capacity are found in many organisms. These nonautonomous mobile elements are commonly referred to as MITEs (miniature inverted transposable elements). First recognized as a predominant sequence type in plants, MITEs have been subsequently identified in many invertebrate and vertebrate genomes (14). A few MITE families have been characterized in archaeal genomes (5, 34) and in eubacteria. *Streptococcus pneumoniae* contains ~100 copies of a 107-bp-long miniature insertion sequence called the repeat unit of pneumococcus (RUP) (29). The 106- to 158-bp-long DNA elements known as Correia or neisseria miniature insertion sequences (NEMIS) make up 1 to 2% of the genome in pathogenic neisseriae (6, 10, 22, 24). RUP and NEMIS feature similar TIRs, and both induce the duplication of the TA dinucleotide upon genomic insertion. Most NEMIS are cotranscribed with neighboring genes, and NEMIS-positive mRNAs fold into hairpins formed by NEMIS termini, which are targeted by RNase III (9, 11). Genome-wide analyses carried out in silico predict that the expression levels of 80 to 100 *Neisseria meningitidis* genes may be tuned by RNase III-dependent processing at NEMIS RNA hairpins (10, 11).

The 127-bp-long elements known either as intergenic repeat units (38) or as enterobacterial repetitive intergenic consensus sequences (ERICs) (17) structurally recall NEMIS and RUP repeats. ERIC families are made up by 20 to 30 elements in both *Escherichia coli* and *Salmonella enterica* serovar Typhimurium. In this report, we show that ERICs, as anticipated by early genomic analyses by Bachellier and coworkers (3), are overrepresented in yersiniae. In silico analyses performed on the wholly sequenced *Yersinia pestis* CO92 (12, 30) and *Yersinia enterocolitica* 8081 (www.sanger.ac.uk/Projects/Y_enterocolitica) strains establish that ERICs constitute a major DNA family in yersiniae. ERICs are (or have been) mobile DNA sequences which also belong to the MITE superfamily. Most of the 247 elements found in *Y. enterocolitica* are inserted at close distance from flanking coding regions, and it is likely that many are transcribed into mRNA. In this paper, we show that, according to their orientations and relative positions within the mRNA, transcribed ERICs may impede or accelerate the decay of specific mRNA segments.

* Corresponding author. Mailing address: Dipartimento di Biologia e Patologia Cellulare e Molecolare, Facoltà di Medicina, Università Federico II, Via S. Pansini 5, 80131 Napoli, Italy. Phone: 0039-81-7462059. Fax: 0039-81-7703285. E-mail: dinocera@unina.it.

MATERIALS AND METHODS

Bacterial strains and growth conditions. The *Y. enterocolitica* strain Ye161 (serogroup O8) was kindly provided by Ida Luzzi at the Istituto Superiore di Sanità, Rome. The *Y. enterocolitica* strains Ye24 (serogroup O8) and Ye25

TABLE 1. Oligonucleotides used to monitor ERIC-positive RNAs[a]

Primer	Sequence
pex. cheW	TTCGTGACGGTTGCTAGTCCTGCCA
pex. trpB	CCCGAACTCGCCAAAATAGGGATTC
pex. uncE	CGATAAAGAACTGTGTACGCAGCAG
pex. lpdA	GGATACAACCGACATTCAGGCACAC
cheB-for	atttaggtgacactatagaaAACTATCAGGTGCGTATTCATGATG
cheB-rev	taatacgactcactatagggGCTTCGTTTTGTGCAATGGTATAAG
cheY-for	atttaggtgacactatagaaTGGTAGACGATTTTTCGACCATGCG
cheY-rev	taatacgactcactatagggTCGGCATGTTCCAGTCAGAAACCAC
panB-for	atttaggtgacactatagaaGCTAACCAGCTATTGAAAGATGCTC
panB-rev	taatacgactcactatagggGAATATACAGCTTAATGGCAGCACG
panC-for	atttaggtgacactatagaaATTGAAACTTTGCCACTGTTACGCC
panC-rev	taatacgactcactatagggATACTCACGACGACAACATCGGCAC

[a] The oligonucleotides used as primers in RNA extension assays are listed at the top. The pairs of 45-mers shown at the bottom have been used to obtain by PCR DNA amplimers in which copies of the bacteriophage T7 promoter (underlined residues) direct the synthesis of antisense RNA probes (Fig. 6). Uppercase residues mark *Y. enterocolitica* sequences.

(serogroup O9) and the *Y. kristensenii* SS47 strain were provided by Francesca Berlutti at the Istituto di Igiene of the University La Sapienza, Rome. *Yersinia* cells were grown in LB broth at 28°C. When needed, exponentially growing Ye161 cells were exposed either for 12 min to rifampin (final concentration, 200 μg/ml) or for 30 min to chloramphenicol (final concentration, 50 μg/ml) before harvesting.

RNA analyses. Total bacterial RNA was purified on an RNeasy column (QIAGEN). Transcripts spanning the *cheW* (open reading frame [ORF] YE2576), *trpB* (ORF YE2213), *uncE* (ORF YE4221), and *lpdA* (ORF YE0702) genes were monitored by RNA extension analyses as reported previously (9) by using as primers the pex.cheW, pex.trpB, pex.uncE, and pex.lpdA oligonucleotides, respectively. The sequences of the four primers are reported in Table 1. Reverse transcriptase-PCR (RT-PCR) analyses were carried out by reverse transcribing 200 nanograms of total *Y. enterocolitica* RNA by random priming. The resulting cDNA was amplified by using pairs of gene-specific oligonucleotides (Table 2). The melting temperature (T_m) of each oligomer (Table 2) was determined by using the Oligo 4.0 primer analysis software (35). In several instances, RT-PCR coamplifications were carried out with alternative pairs of primers. One oligonucleotide of each pair had been ^{32}P end labeled at the 5′ terminus with the polynucleotide kinase. Comparable yields of amplimers were obtained by labeling either forward or reverse cistron-specific primers. To adequately monitor gene-specific RNA levels by RT-PCR, the cDNA was amplified under nonsaturating cycling conditions, and ad hoc low-cycle-number (6 to 12 cycles) PCR analyses were performed for each set of coamplified genes. Amplimers were electrophoresed onto 6% polyacrylamide-8 M urea gels and quantitated by phosphorimagery.

For RNase protection assays, uniformly ^{32}P-labeled RNA probes were obtained by transcribing in vitro linear DNA templates as described previously (9). Templates were obtained by PCR amplification of Ye161 DNA with the 45-mers shown in Table 1. Within each pair, one oligomer included the sequence of the T7 RNA polymerase promoter in the 5′ region. Twenty micrograms of total RNA were mixed with ^{32}P-labeled antisense RNA probes in 30 μl of hybridization buffer (75% formamide, 20 mM Tris [pH 7.5], 1 mM EDTA, 0.4 M NaCl, 0.1% sodium dodecyl sulfate). Samples were incubated at 95°C for 5 min, cooled down slowly, and kept at 45°C for 16 h. After a 60-min incubation at 33°C with RNase T_1 (2 μg/ml), samples were treated with proteinase K (50 μg/ml) for 15 min at 37°C, extracted once with phenol, precipitated with ethanol, resuspended in 80% formamide, and loaded onto 6% polyacrylamide-8 M urea gels.

Computer analysis. *E. coli* ERIC sequences were used as queries in BLAST searches (2) to fetch homologous DNA segments from the genomes of the *Y. pestis* CO92 (30) and KIM (12) strains and from *Y. enterocolitica* 8081 (www.sanger.ac.uk/Projects/Y_enterocolitica). Species-specific queries allowed the identification of *Yersinia* ERICs evolutionarily distant from *E. coli* homologs. Retrieved DNA sequences were aligned with the CLUSTAL W program (41). Consensus sequences from multiple alignments of ERIC family members were established with the program CONS of the EMBOSS package. Secondary structure modeling was done using the Mulfold program (www.bioinfo.rpi.edu/applications/mfold), which predicts RNA secondary structure by free-energy minimization (45).

RESULTS

Genomic and structural organization of ERICs in yersiniae. The genus *Yersinia* includes 11 species, 3 of which are pathogenic to humans (4). The enteropathogens *Y. pseudotuberculosis* and *Y. enterocolitica* are widely found in the environment. In contrast, *Y. pestis* is a highly virulent blood-borne pathogen which is transmitted by fleas and which rapidly evolved from *Y. pseudotuberculosis* (1, 44). In silico analyses carried out on wholly sequenced strains showed that *Yersinia* chromosomes are peppered by ERIC repeats. By looking only at elements carrying both TIRs (Fig. 1), we found 247 and 167 ERICs in the genomes of the *Y. enterocolitica* 8081 and *Y. pestis* CO92 strains, respectively (Table 3). About 90% of the elements are scattered throughout the chromosome of either species as single-copy insertions. The remaining 10% is made up by clusters in which two to five elements are organized in head-to-tail configuration. On the whole, 235 and 151 ERIC-positive sites were identified in Y. *enterocolitica* 8081 and Y. *pestis* CO92 strains, respectively (Table 3). In contrast, the *Y. pestis* CO92 strain contains several moderately abundant families of insertion sequences (ISs) (65 copies of IS*1541*, 44 copies of IS*100*, 8 copies of IS*1661*, and 21 copies of IS*285*; see reference 7), while we found only 3 copies of IS*1541* in the Y. *enterocolitica* 8081 genome by BLAST analyses (not shown).

Unit-sized ERICs are 127 bp in length (Fig. 1). Shorter elements measure ~70 bp, and all lack a 50-bp-long internal segment. Larger elements are interrupted at specific sites by three different types of DNA insertions (Fig. 1). Type 1 and type 2 insertions have been found also in some *E. coli* ERICs (37), while type 3 insertions seem to be present only in yersiniae.

Y. pestis and *Y. enterocolitica* genomes both measure ~4.6 Mb. However, extensive genetic remodeling makes *Y. pestis* a species evolutionarily distant from other yersiniae (44). *Y. pestis* ERICs are fewer and exhibit more size heterogeneity than *Y. enterocolitica* elements (Fig. 1A). The *Y. pestis* CO92 and the *Y. enterocolitica* 8081 chromosomes share only 37 syntenic regions carrying ERIC repeats. Elements have the same size only in one-third of the cases. In the other instances, unit-length elements found in *Y. pestis* are replaced by either shorter or insertion-tagged ERICs in *Y. enterocolitica*, and vice versa (not shown), plausibly as a result of recombination events between ERIC family members.

The insertion of ERIC induces a 2-bp target site duplication. Several syntenic regions identified in *Y. enterocolitica* and *Y. pestis* carry an ERIC element in the former species only. ERICs terminate at either side with the dinucleotide TA. At many *Y. pestis* empty sites, ERIC is replaced by one copy of the dinucleotide (Fig. 2). The duplication of the dinucleotide TA is a hallmark of eukaryotic MITEs and is a feature shared by known eubacterial MITEs (24, 29). TA empty sites have been identified both in *Y. enterocolitica* and in *Y. pestis* (Table 3). This indicates that the mobilization of ERICs still occurred after the speciation of yersiniae into *Y. enterocolitica* and *Y. pseudotuberculosis*, from which *Y. pestis* eventually derived (1, 44).

Differences in the distributions of ERICs between the *Y.*

TABLE 2. Oligonucleotides used for PCR and RT-PCR analyses

Gene	Primer[a]			
	Direct		Reverse	
	Sequence	T_m (°C)	Sequence	T_m (°C)
cheW	CGAAACGGTAGGACAAGAATTCCTG	59.1	GGAACAATAACGCCGCGTAAGTTAG	59.2
cheA	TCATTTTACCATTGAACGCCGTAAT	57.7	CAGAAATACCTGGAACCTTGCGATA	57.5
cheA	AGGCATTGTTGTGATTCTACAAAGC	55.7	ACGACTCCATCATCAGCCGTAACAC	60.2
trpC	TTGAACGCTATGTTTTGGATAATGG	56.3	CAATCTTTTGGGGATCTTTAATGCC	58.1
trpB	ATCCCTATTTTGGCGAGTTCGGGGG	56.2	CAGAGCGGTTGGACGCCCAGCATAG	58.0
phoU	CATATTTCCGGCCAGTTCAATGCAG	62.3	CTTTTTATCACCCTCGATGACGCGC	63.5
phoT	GTTATAGCTTGTCGGGTGGGCAGCA	63.9	TTCTGCTGTGGTGCGGTAAACAGGG	64.8
phoT	AGGTATCGCCATTCGTCCAGATGTG	62.0		
cheY	TGGTAGACGATTTTTCGACCATGCG	62.8	TCGGCATGTTCCAGTCAGAAACCAC	63.0
cheB	AACTATCAGGTGCGTATTCATGATG	64.2	GCTTCGTTTTGTGCAATGGTATAAG	66.2
cheB	AATTACCGTGAAGGAAGCAGAAGAC	66.2		
glgA	CGTATGTTCTGAGCTATTCCCGTTG	58.1	AGCAAAGGTATCAATCTCCCTGACC	57.9
glgA	TACGGCATGGAGGGGTTGCTACAAG	60.5	AAGCCATACAACTGTGTTAGCCCAC	57.5
glgC	GTAGCCACGGTATGACCATGAACTC	57.7	GCAGCAGTAATGTGGAATCAATGGT	58.2
glgC			GATAAAAACGCTTGCTGTCTTCTTC	55.0
manX	GCAATATGCCAAAGACCGGGTCATG	64.0	TTCGGACTTCCAGTTCAATACCGCG	63.9
manY	ATTTCATCGTTGCCTGTATCGCCGG	63.7	ACCAAAGTACAGGCGACGAGGGGAC	64.1
manY			CAGCCGAGCGCGATCATTTCTAAGG	65.5
panB	GCTAACCAGCTATTGAAAGATGCTC	54.9	GAATATACAGCTTAATGGCAGCACG	56.3
panC	ATTGAAACTTTGCCACTGTTACGCC	59.5	ATACTCACGACGACAACATCGGCAC	61.0
pstS	TGCGGCAAAAGGTGTAGACTGGAGC	64.2	AATCTGAGTTTTCCAGGCAGCACGG	63.3
pstC	ATAAGCCGACAATCAAAGCACCGAG	61.4	CCACAGGAAAGCCCAACCAAATTTC	62.5
argB	TGGCAGTCTGATGAACGTAAATGCC	61.1	CATTCACTTTAACCACCATGCCGTC	60.4
argH	TCAGGCGGCAGATCAGCGTTTTAAG	64.2	GTTGCTGTTCGGCCGTCGTTAAAAC	63.4

[a] In some instances, the level of cistron-specific transcripts was monitored by using novel primers.

pestis CO92 and *Y. enterocolitica* 8081 genomes reflect species-specific, rather than strain-specific, variations. The *Y. pestis* strains CO92 (30) and KIM (12) belong to different biovars, have been responsible for the spreads of different plague epidemics, and show a remarkable amount of genome rearrangement (12). However, 155/157 ERIC-positive sites found in the CO92 strain are perfectly conserved, as revealed by BLAST analyses, in the KIM strain, and the remaining two sites vary only in terms of the number of tandemly inserted elements.

ERICs are cotranscribed with flanking genes. Genome-wide surveys revealed that 137 ERICs are inserted at close distance (≤50 bp) from either the start or the stop codons of *Y. enterocolitica* 8081 ORFs (not shown). This suggests that most elements are cotranscribed with flanking genes into mRNAs.

To investigate the issue, we first checked that ERIC-positive regions found in the 8081 strain were conserved in the *Y. enterocolitica* Ye161 strain. Subsequently, the corresponding ERIC-positive mRNAs synthesized in this strain were monitored by primer extension analyses (Fig. 3). The major products of extension of both *lpdA* and *uncE* transcripts extended beyond ERIC (Fig. 3). In contrast, extension products of both *cheW* and *trpB* transcripts were found to terminate at multiple sites within ERIC sequences (Fig. 3). The same pattern was obtained with different RNA preparations and reverse transcriptase batches. The multiple extension products detected may denote cleavage of *cheW* and *trpB* mRNAs at ERIC sequences.

ERICs flanking the *lpdA* and *uncE* genes are both inserted in the same orientation, which from here on we will arbitrarily refer to as the A orientation. In contrast, elements flanking the *cheW* and *trpB* genes are inserted in the alternative B orientation. About 110 ERICs are found, within a −50- to +45-bp distance range, downstream from the stop codons of annotated ORFs in the 8081 strain (Fig. 4). Curiously, most ERICs which either overlap or are inserted next to (0- to +6-bp distance range) stop codons are B-oriented elements. In contrast, ERICs located at larger distances from ORFs are predominantly A-oriented elements (Fig. 4). The orientation dependence rule works for elements located between unidirectionally transcribed ORFs as for elements separating convergently transcribed ORFs. A privileged orientation relative to the distance from translational stop codons was similarly displayed by ERICs found in the *Y. pestis* CO92 strain (not shown).

To investigate the functional significance of these observations, several pairs of *Y. enterocolitica* genes transcribed in the same direction, but separated by either A- or B-oriented ERICs, were selected for comparative RNA quantitations. Elements analyzed measured all 127 bp and exhibited 94% sequence similarity. Total RNA from Ye161 cells was reverse transcribed into cDNA, and the latter was subsequently am-

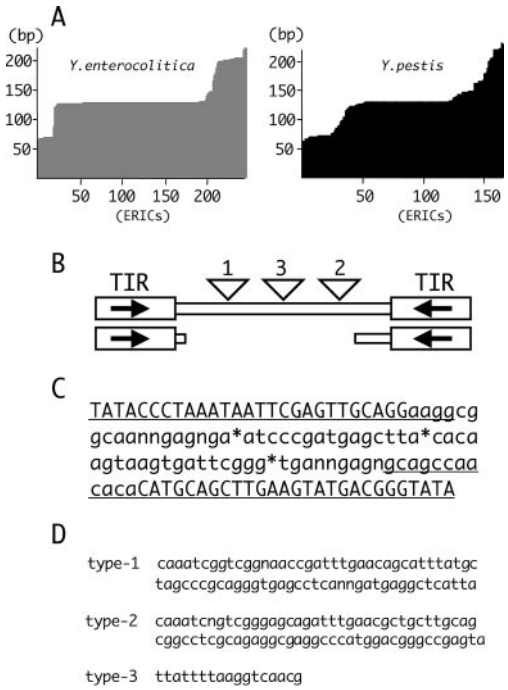

FIG. 1. ERIC elements in yersiniae. (A) ERIC-sized classes in *Y. enterocolitica* 8081 and *Y. pestis* CO92 strains. The number of elements carrying both TIRs found and their sizes in base pairs are indicated. (B) Structural organization of ERICs. Boxed arrows mark the TIRs. Triangles mark type 1-to-type 3 insertions interrupting ERIC sequences. (C) The consensus sequence of the 127-bp unit-length ERICs is shown in the A orientation. TIR residues are in capital letters. Underlined residues mark sequences conserved in the internally rearranged 70-bp-long ERICs. The integration sites of type 1-to-type 3 insertions are denoted by asterisks. (D) The consensus sequences of the three types of intervening sequences found to interrupt ERICs are shown.

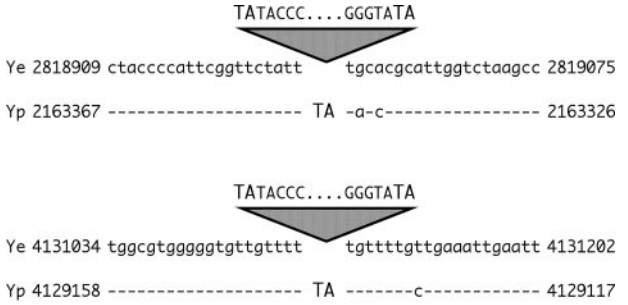

FIG. 2. Filled and empty ERIC sites. Homologous DNA regions from the *Y. enterocolitica* 8081 (Ye) and *Y. pestis* CO92 (Yp) strains are aligned. Numbers refer to genome residues; dashes denote sequence identities. The duplication of the TA target site at ERIC termini is highlighted.

plified by using different sets of primers. As evidenced by the detection of large mRNA segments, elements selected are cotranscribed with flanking genes (Fig. 5A). To monitor the relative abundances of RNA species corresponding to upstream and downstream cistrons, the cDNA was coamplified with pairs of cistron-specific oligomers (Table 2) under nonsaturating cycling conditions (Fig. 5B). Radiolabeled amplimers were separated electrophoretically, and their amounts were quantitated by phosphorimagery. Data obtained with alternative sets of primers were fairly comparable, ruling out technical artifacts. By looking at transcriptional units spanning B-oriented ERICs, we found that downstream gene transcripts accumulated ~4-fold more abundantly than upstream gene transcripts. In contrast, except for the *glgC-glgA* barrier, the levels of gene transcripts flanking A-oriented ERICs were comparable (Fig. 5C). Differences in the downstream/upstream gene transcript ratios measured at intercistronic barriers carrying A-oriented (*panB-panC*) and B-oriented (*cheY-cheB*) ERICs were confirmed by RNase protection experiments and magnified when de novo RNA synthesis was blocked by treating *Yersinia* cells with rifampin (Fig. 6). Both *panB* and *panC* transcripts, which are quite abundant in steady-state RNAs, were no longer detected after exposure of *Y. enterocolitica* cells to rifampin (Fig. 6B, compare lanes 20 and 21). By contrast, the difference in the steady-state levels of *cheY* and *cheB* transcripts made it still possible to detect *cheY* RNA sequences in rifampin-treated cells (Fig. 6A, compare lanes 9 and 10).

Data signal that the segmental stabilities of RNAs spanning A-oriented and B-oriented elements were substantially different.

TABLE 3. ERIC elements in wholly sequenced *Y. enterocolitica* 8081 and *Y. pestis* CO92 strains

ERIC element or copy no.	No. in:	
	Y. enterocolitica 8081	*Y. pestis* CO92
Copy no.	247	167
ERIC$^+$ sites	235	151
Single-copy inserts	225	148
Type I insertions	13	11
Type II insertions	12	2
Type III insertions	5	35
TA empty sites	23	3

Heterogeneity of ERIC-positive loci among yersiniae. The conservation of ERIC sequences in *Y. enterocolitica* was monitored by PCR-driven surveys. The Ye161 and Ye24 strains and the sequenced 8081 strain all belong to the O8 serogroup. It is therefore not surprising that 24/24 ERIC-positive loci analyzed (including those shown in Fig. 5) were conserved in the three strains (data not shown). In contrast, genetic variations at specific loci spanning ERIC sequences found in the 8081 strain were identified in Ye25, a serogroup O9 *Y. enterocolitica* strain, as well as in the YkSS47 strain of the apathogenic *Yersinia kristensenii* species and exploited for comparative RNA analyses. In Ye161, *cheA* and *cheW* genes are separated by a B-oriented ERIC, and *cheW* transcripts are ~5-fold more abundant than *cheA* transcripts. The difference is abolished in YkSS47 cells (Fig. 7). Sequence analysis showed that the YkSS47 *cheA-cheW* region did not experience the insertion of ERIC DNA. In Ye161, *argB* and *argH* genes are separated by a B-oriented ERIC inserted immediately downstream from the *argB* stop codon. In Ye25, in contrast, the two genes are separated by an A-oriented ERIC inserted 10 bp downstream from the *argB* stop codon. Changes in the position and the orientation of ERIC are associated with significant differences

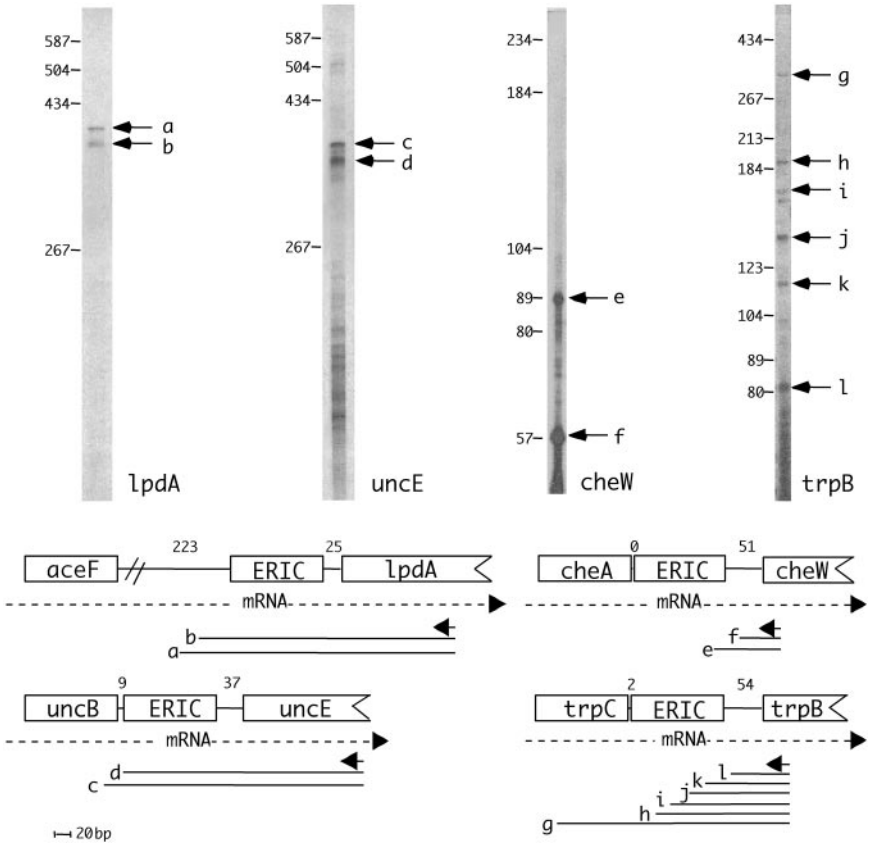

FIG. 3. Primer extension analyses of ERIC-positive transcripts. Primers that had been ^{32}P labeled at the 5′ end and were complementary to *lpdA*, *uncE*, *cheW*, and *trpB* transcripts were hybridized to total RNA (5 μg) derived from the *Y. enterocolitica* Ye161 strain. Annealed primer moieties were extended in the presence of nucleoside triphosphates by avian myeloblastosis virus reverse transcriptase. Reaction products were electrophoresed on 6% polyacrylamide-8 M urea gels. Major reaction products labeled "a" to "l" are marked by arrows. Numbers to the left of each autoradiogram refer to the size in nucleotides of coelectrophoresed DNA molecular size markers. In the diagrams at the bottom are sketched the organizations of the ERIC-positive regions analyzed. The direction of transcription of the genes analyzed is indicated by dotted arrows. Primers are denoted by arrows; lines labeled "a" to "l" denote the extended products. Numbers indicate the distances in base pairs separating ERICs from either the stop or the start codons of neighboring ORFs.

in the *argH-argB* transcript ratios (Fig. 7). Finally, the ERIC which separates *panB* and *panC* genes in Ye161 is missing in the YkSS47 strain. This correlates with a threefold decrease in the level of the *panB* transcripts (Fig. 7).

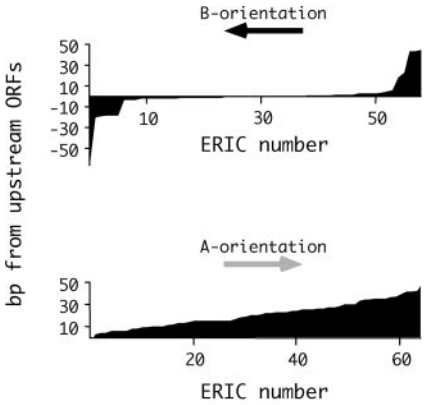

FIG. 4. Asymmetry in the orientations of ERICs. The distances in base pairs separating B-oriented and A-oriented ERICs from flanking upstream ORFs in the *Y. enterocolitica* 8081 strain are indicated.

Translating ribosomes and RNA folding. Data shown in Fig. 5 to 7 support the notion that the relative abundance of the mRNA segments flanking ERIC sequences may be influenced by the orientation of ERICs. The high downstream/upstream transcript ratio measured at intercistronic barriers spanning B-oriented elements may correlate with the activity of promoter sequences directing the synthesis of transcripts toward downstream genes. In A-oriented ERICs, the hypothetical promoter would also direct the synthesis of transcripts toward upstream genes, causing transcriptional collisions and allowing for the formation of antisense RNA. It is difficult to envisage how this may be advantageous to the organism. Moreover, it is left unexplained why B-oriented elements tend to be inserted so close to stop codons. We rather believe that transcribed ERICs may act as modulators of RNA decay and that A- and B-oriented elements may function in different ways. According to this hypothesis, the high downstream/upstream gene transcript ratios measured at intercistronic barriers carrying B-oriented ERICs may be the result of processing events promoted by ERIC repeats which enhance upstream RNA degradation.

The orientation-dependent mode of action suggests that a

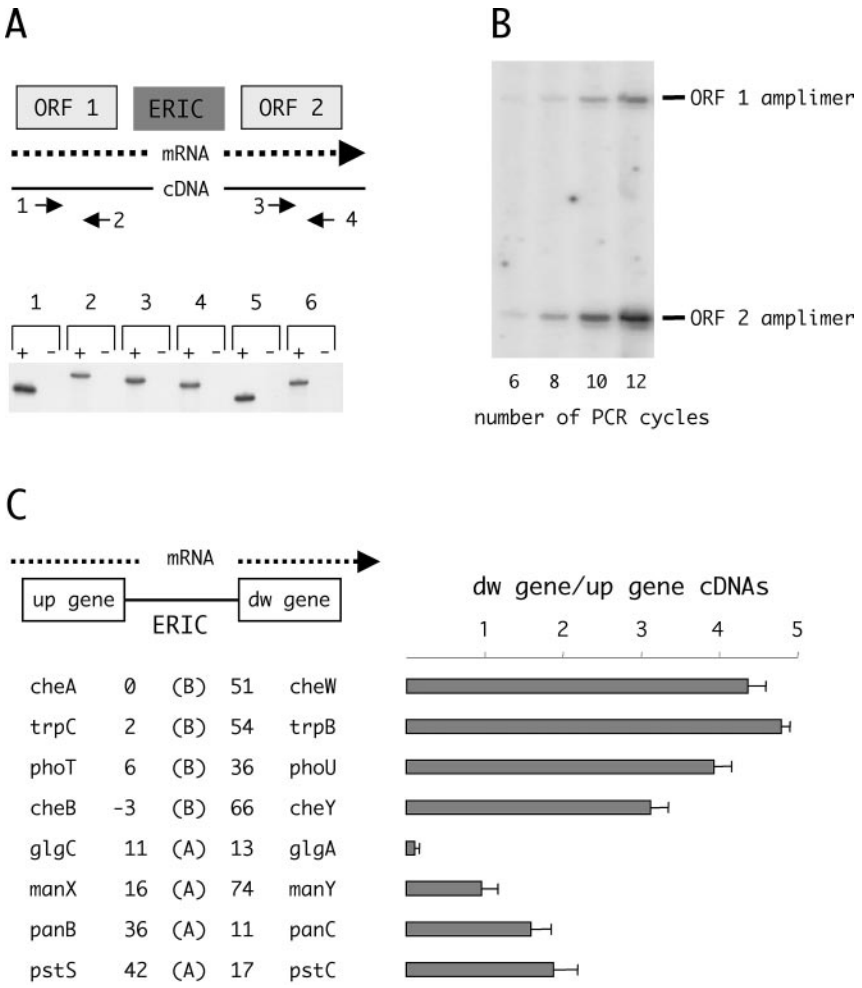

FIG. 5. RT-PCR analyses of ERIC-positive transcripts. Total RNA (200 nanograms) derived from the Ye161 strain had been reverse transcribed by using a mixture of random hexamers as primers. The cDNA obtained had been amplified by PCR with cistron-specific oligomers. One oligonucleotide of each pair of primers was ^{32}P end labeled to allow amplimer detection by autoradiography. Reaction products were run on 6% polyacrylamide-8 M urea gels. (A) Transcripts spanning ERIC sequences and *cheA-cheW* (lane 1), *cheB-cheY* (lane 2), *manX-manY* (lane 3), *panB-panC* (lane 4), *trpC-trpB* (lane 5), and *pstS-pstC* (lane 6) genes were detected by using external primers 1 and 4 under standard PCR cycling conditions (20 to 22 cycles). Amplimers were detected only when RNA samples were incubated with reverse transcriptase (+ lanes) prior to PCR. (B) Total cDNA from the Ye161 strain had been amplified by using pairs of ORF-specific primers for a limited number of PCR cycles (6 to 12). Amplimers were quantitated by phosphorimaging. In the example reported, amplimers 1 and 2 correspond to the *cheA* and *cheW* genes, respectively (C) The listed genes flanking ERIC repeats have been analyzed as described above. Distances in base pairs separating ERIC termini from stop and start codons of flanking ORFs are indicated. The orientation of the ERIC (A or B) is given in parenthesis. The number of transcripts corresponding to downstream (dw) and upstream (up) genes for each pair is expressed as a ratio. RT-PCR analyses were routinely repeated three to four times on two independent RNA preparations. Standard deviations are indicated. For each ORF analyzed (with the YE number assigned by the Sanger Centre shown in parentheses), the hypothesized function, system, and/or product(s) are as follows: for *cheA* (YE2577), chemotaxis protein CheA; for *cheW* (YE2576), chemotaxis protein CheW; for *trpC* (YE2212), tryptophan biosynthesis bifunctional protein; for *trpB* (YE2213), tryptophan synthase subunit B; for *phoT* (YE4198), high-affinity P-specific transport and cytoplasmic ATP-binding protein; for *phoU* (YE4196), P uptake, high-affinity P-specific transport system, and regulatory gene; for *cheB* (YE2571), glutamate methylesterase; for *cheY* (YE2570), chemotaxis protein CheY; for *glgC* (YE4011), glucose-1-phosphate adenylyltransferase; for *glgA* (YE4010), glycogen synthase; for *manX* (YE1777), mannose phosphotransferase system and EIIAB component; for *manY* (YE1776), mannose phosphotransferase system and EIIC component; for *panB* (YE0720), ketopantoate hydroxymethyltransferase; for *panC* (YE0719), pantoate-beta-alamine ligase; for *pstS* (YE4201), phosphate-binding periplasmic protein; and for *pstC* (YE4200), phosphate transport system permease.

sequence must be crucial for upstream RNA instability. RNAs corresponding to A-oriented and B-oriented ERICs may fold into secondary structures which have similar shapes and comparable calculated free energies (Fig. 8A; see references 17 and 38). The formation of RNA hairpins is preserved in the majority of elements by compensatory mutations and is unaffected in shorter as well as larger ERICs, because both type 1 and type 2 insertions feature self-complementary regions (Fig. 1D; see also reference 37). However, the left-hand TIRs of ERICs, which are inserted close to stop codons, are covered by terminating ribosomes, a translating ribosome protecting at least 30 residues of the mRNA (40). It is noteworthy that an AU-rich sequence (AAUUAUUUA; Fig. 8A) would not be base paired in B-oriented elements because of steric hindrance

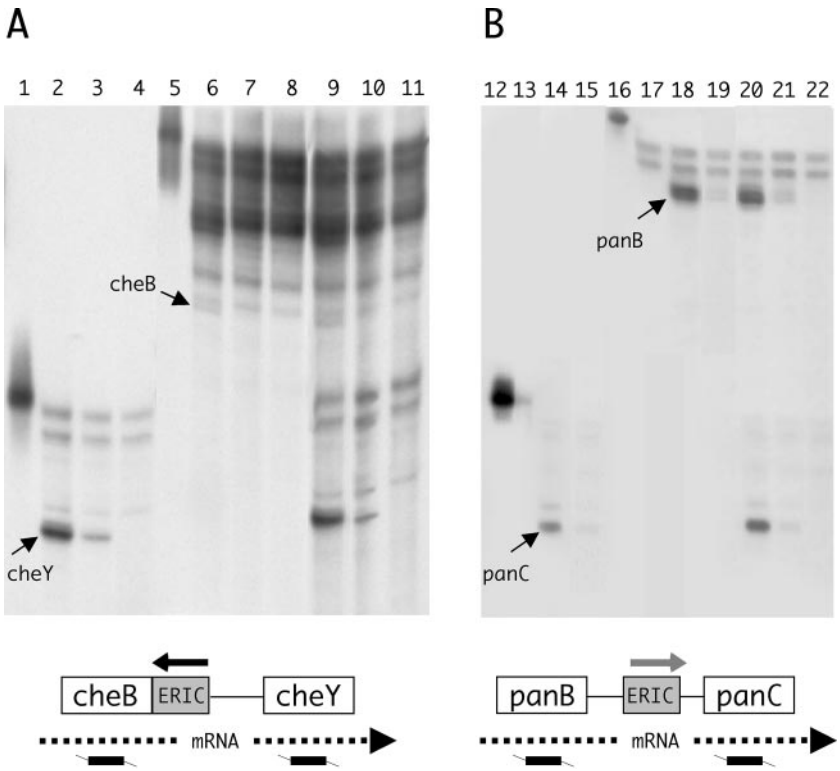

FIG. 6. RNase protection of ERIC-positive transcripts. Uniformly ^{32}P-labeled antisense RNA probes, complementary to the coding regions of the *Y. enterocolitica cheB-cheY* and *panB-panC* genes, were transcribed in vitro by the T7 RNA polymerase. In the diagram, RNA probes are sketched (not to scale) below the gene depictions. Thicker segments mark complementarity to mRNA. Probes were hybridized to 20 μg of total RNA from Ye161 cells untreated or exposed to rifampin (final concentration, 200 μg/ml) for 12 min before cell harvesting. RNase T_1-resistant RNA hybrids were electrophoresed on 6% polyacrylamide-8 M urea gels. Reaction products corresponding to *cheY*, *cheB*, *panC*, and *panB* RNAs are marked by arrows. (A) Analysis of *cheB-cheY* RNAs. Lanes: unreacted input probes (1, *cheY*; 5, *cheB*); probes hybridized separately to total RNA from Ye161 cells untreated (2, *cheY*; 6, *cheB*) or exposed for 12 min to rifampin (3, *cheY*; 7, *cheB*) or hybridized to *E. coli* tRNA (4, *cheY*; 8, *cheB*). Probes were hybridized together to total RNA from Ye161 cells untreated (9) or exposed for 12 min to rifampin (10) or hybridized to *E. coli* tRNA (11). (B) Analysis of *panB-panC* RNAs. Lanes: unreacted input probes (12, *panC*; 16, *panB*); probes hybridized separately to total RNA from Ye161 cells untreated (14, *panC*; 18, *panB*) or exposed for 12 min to rifampin (15, *panC*; 19, *panB*) or hybridized to *E. coli* tRNA (13, *panC*; 17, *panB*). Probes were hybridized together to total RNA from Ye161 cells untreated (20) or exposed for 12 min to rifampin (21) or hybridized to *E. coli* tRNA (22).

caused by ribosomes. Unfolded AU-rich sequences represent preferred cleavage sites for RNase E (13, 19, 21, 26). The enzyme, which is conserved both in *Y. enterocolitica* and *Y. pestis* (ORFs YE1627 and YPO1590, respectively), is the major endoribonuclease responsible for the mRNA decay in bacteria (8) and is associated in *E. coli* with the 3′-5′ exoribonucleases polynucleotide phosphorylase and RNase II in the molecular machine known as degradosome (8, 32). The mRNA degradation by 3′-5′ exonucleases subsequent to RNase E-mediated cleavage may explain the high downstream/upstream transcript ratios measured at specific ERIC-positive intercistronic barriers (Fig. 5 to 7).

Experimental support to this hypothesis is provided by data shown in Fig. 8B. Cleavage of ERIC-positive mRNAs should be favored by the occupancy of the left-hand ERIC TIR by translating ribosomes. Moreover, uncoupling transcription and translation should alter the downstream/upstream gene transcript ratio in ERIC-positive mRNAs spanning B-oriented ERICs only. ERICs located downstream from the *cheA* and *panB* genes are inserted in the B and A orientations, respectively (Fig. 5). Treatment of Ye161 cells with chloramphenicol significantly altered the *cheW-cheA* transcript ratio, as we measured a fourfold increase in the amount of *cheW* RNA but no effect on the *panC-panB* transcript ratio (Fig. 8B; see references 23 and 39).

It is noteworthy that the predominant extension products corresponding to the "e" and "l" bands in Fig. 3 nicely match in size RNA species generated by cleavage of *cheW* and *trpB* transcripts, respectively, at the AU-rich site within the upstream B-oriented ERICs.

A-oriented ERICs are found far from stop codons and therefore can fold into RNA hairpins. These elements may therefore act in a way opposite from that of to B-oriented ERICs and function as upstream RNA stabilizers (see Discussion).

DISCUSSION

Origin and evolution of ERIC sequences. ERIC repeats are present in several bacterial species as low-copy-number families, and PCR fingerprinting using ERIC primers is widely used for diagnostic purposes (43). In contrast, ERICs are a major genome component in pathogenic yersiniae, accounting for ~0.7% and ~0.45% of the total DNA contents of *Y. enterocolitica* and *Y. pestis*, respectively. In either species, elements

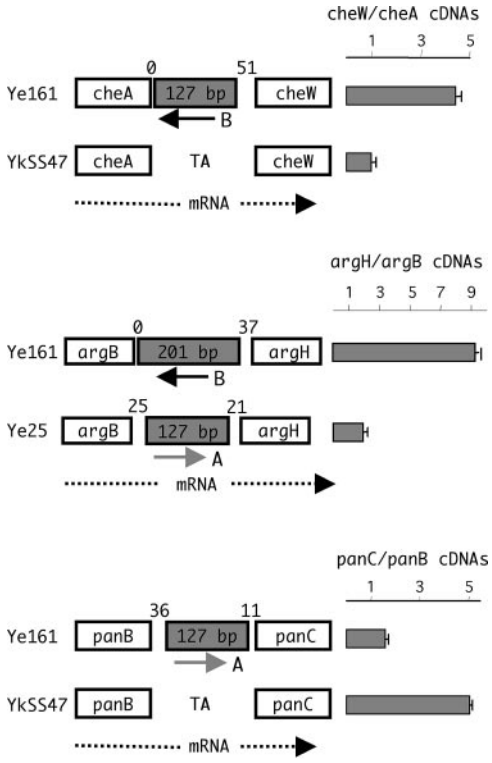

FIG. 7. Comparison of loci carrying or missing ERIC sequences in different *Yersinia* strains. ERIC elements are depicted as gray boxes, and numbers within refer to element sizes. Numbers above boxes signal the distances in base pairs separating ERIC from flanking ORFs. Total RNAs derived from *Y. enterocolitica* strains Ye161 and Ye25 and from *Y. kristensenii* strain YkSS47 were analyzed by RT-PCR as described for Fig. 5. At the empty genomic sites identified in the genome of the YkSS47 strain, ERIC sequences are replaced by the dinucleotide TA.

are scattered throughout the chromosome mostly as single-copy insertions. The genomic spread of ERICs occurred most probably by transposition. As unambiguously set by the comparison of empty and filled chromosomal sites, ERICs specifically duplicate the dinucleotide TA upon genomic insertion (Fig. 2). This is a hallmark of miniature transposable elements originating from members of the IS*630*-Tc1-mariner TE superfamily known as MITEs. The mobilization of ERICs, initially fostered by large codogenic progenitor ISs, also might have been eventually mediated, as has been previously suggested for eukaryotic MITEs (15, 18, 31, 36), by ISs whose transposases were able to recognize ERIC termini. ERICs are plausibly no longer mobile in yersiniae, as we could identify in silico neither bona fide ERIC progenitors nor potential cross-mobilizing TEs either in the sequenced *Y. enterocolitica* and *Y. pestis* strains or in the genome of the *Y. pseudotuberculosis* IP32593 strain, whose sequence has been recently determined (7). Data reported in this work support the notion that yersiniae learned during evolution to exploit the genomic spread of ERICs for functional purposes.

ERICs as modulators of RNA decay. In yersiniae, ERICs are frequently inserted next to codogenic regions, and most are plausibly transcribed into mRNAs. The ability of ERIC RNA to fold into relatively robust, low-free-energy RNA hairpins (Fig. 8A) is a feature previously noted (17, 38).

Whole in silico surveys surprisingly revealed a privileged orientation of ERIC sequences relative to their position in the mRNA. In the *Y. enterocolitica* 8081 strain, 56/60 elements which either overlap or are located 6 bp or less from the stop codon of annotated ORFs are inserted in the same orientation (B-oriented ERICs). By contrast, 45/47 elements located more distantly from stop codons (distance range, +7 to +35) are inserted in the opposite orientation (A-oriented ERICs). This peculiar organization must convey a selective advantage in evolution for functional purposes.

The preferential location next to stop codons implies that RNA hairpins formed by B-oriented ERICs are remodelled by terminating ribosomes (Fig. 8C). We hypothesize that inhibiting secondary structure formation unmasks a potential target site for RNase E, which is located in the right-hand TIR of these elements. In turn, the endonucleolytic cleavage activates the degradation of upstream RNA segments by polynucleotide phosphorylase and RNase II, the two 3′-5′ exoribonucleases associated with the RNase E in the degradosome (8, 32).

Translation should not interfere with the formation of RNA secondary structures in A-oriented ERICs. By folding into stable RNA hairpins, these repeats should be able to slow down the degradation of upstream RNA segments by impeding the passage of 3′-5′ exonucleases. These repeats may thus work analogously to the shorter intergenic sequences known as REPs, which are found in *E. coli* (16). The element found at the *glgC-glgA* intercistronic barrier seems to work this way (Fig. 5). A similar conclusion can be reached for the element found between *panB* and *panC* cistrons (Fig. 7). However, in other transcriptional units spanning A-oriented elements, upstream and downstream transcripts accumulated at similar levels (Fig. 5). We do not have an explanation for such discrepancies. Plausibly, several A-oriented ERICs cannot function as upstream RNA stabilizers because they are overridden by dominant instability determinants located in the mRNA. Such a phenomenon has been documented for different *E. coli* REPs (25, 27, 28). Similarly, the degradation of 5′ flanking RNA prompted by B-oriented ERICs may be impaired by mRNA stability determinants. The efficacy by which ERICs modulate RNA decay may vary not only because of the intrinsic stabilities of neighboring mRNA segments but also because of sequence heterogeneity among ERICs. Thus, conclusions on the abilities of members of the ERIC family to function as RNA control elements can be drawn in many instances only by integrating sequence data with functional RNA analyses.

In spite of the smaller size of their family, *Y. pestis* ERICs also can be largely sorted into A-oriented and B-oriented elements according to their distances from upstream ORFs. Whether the ERIC-dependent modulation of RNA decay works in this species, which rapidly evolved as an arthropod-adapted pathogen, remains to be established.

In the *Y. enterocolitica* 8081 strain, 30 elements are inserted relatively far from ORF stop codons but close (≤50-bp distance) to ORF start codons. These repeats may either stabilize downstream RNA sequences (*lpdA* and *uncE* transcripts in Fig. 3) or interfere with mRNA translation. Some ERICs, alternatively, could function as DNA, rather than as RNA, elements. However, deleting an ERIC from the promoter re-

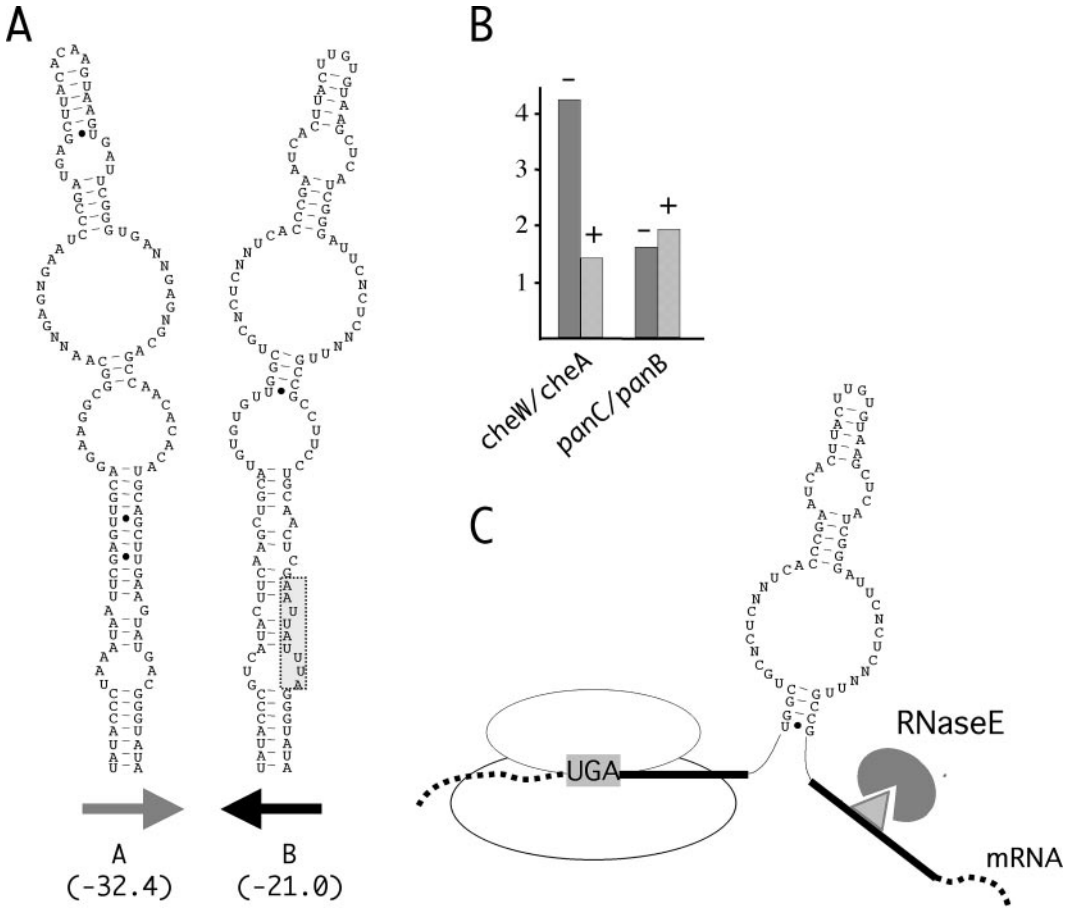

FIG. 8. (A) Predicted RNA foldings and relative calculated free energies at 37°C of unit-length ERIC consensus sequences inserted in A and B orientations. Non-Watson-Crick base pairings are highlighted by dots. The hypothesized cleavage site for RNase E, present in B-oriented ERICs, is boxed. (B) Translation-dependent processing of ERIC-positive RNAs. Total RNA derived from exponentially growing Ye161 cells untreated (−) or exposed for 30 min to chloramphenicol (+) (final concentration, 50 μg/ml) was analyzed as described for Fig. 5. (C) Ribosomes interfere with folding of ERIC-positive RNA. In mRNA-spanning B-oriented elements that are inserted close to the translational stop codon, the translating ribosome covers most of the ERIC left-hand TIR, unmasking the RNase E site (sketched as a triangle) located in the ERIC right-hand TIR.

gion of the *Y. enterocolitica cpdB* gene had no effect on *cpdB* expression (42). By contrast, the ERIC found in the promoter of the *Y. enterocolitica ybtA* yersiniabactin regulator may modulate yersiniabactin activity, as putative binding sites for the YbtA transcriptional regulator and the TATACCC motif found in ERIC TIRs coincide (33).

The numbers, the structural organizations, and the chromosomal distributions of ERICs and neisserial NEMIS sequences are similar. It is curious to note that members of these two MITE families, spread in evolutionarily distant gram-negative bacteria, independently evolved into substrates for the major cellular endoribonucleases. We would not be surprised to learn that bacterial MITEs yet to be discovered may have similarly evolved into *cis*-acting sequences regulating mRNA metabolism. Whether MITE-like repeats found in eukaryotes may similarly work as RNA regulatory elements remains to be established.

ACKNOWLEDGMENTS

We are indebted to Ida Luzzi and Francesca Berlutti for providing us with *Yersinia* strains and to Bruno Bruni for critical revision of the manuscript.

This work has been funded by a grant assigned to Pier Paolo Di Nocera by the PRIN 2004 agency of the Italian Ministry of the University and Scientific Research.

REFERENCES

1. **Achtman, M., K. Zurth, G. Morelli, G. Torrea, A. Guiyoule, and E. Carniel.** 1999. Yersinia pestis, the cause of plague, is a recently emerged clone of Yersinia pseudotuberculosis. Proc. Natl. Acad. Sci. USA **96:**14043–14048.
2. **Altschul, S. F., W. Gish, W. Miller, E. W. Myers, and D. J. Lipman.** 1990. Basic local alignment search tool. J. Mol. Biol. **215:**403–410.
3. **Bachellier, S., J. M. Clement, and M. Hofnung.** 1999. Short palindromic repetitive DNA elements in enterobacteria: a survey. Res. Microbiol. **150:** 627–639.
4. **Bottone, E. J.** 1999. Yersinia enterocolitica: overview and epidemiologic correlates. Microbes Infect. **1:**323–333.
5. **Brugger, K., P. Redder, Q. She, F. Confalonieri, Y. Zivanovic, and R. A. Garrett.** 2002. Mobile elements in archaeal genomes. FEMS Microbiol. Lett. **206:**131–141.
6. **Buisine, N., C. M. Tang, and R. Chalmers.** 2002. Transposon-like Correia elements: structure, distribution and genetic exchange between pathogenic Neisseria species. FEBS Lett. **522:**52–58.
7. **Chain, P. S., E. Carniel, F. W. Larimer, J. Lamerdin, P. O. Stoutland, W. M. Regala, A. M. Georgescu, L. M. Vergez, M. L. Land, V. L. Motin, R. R. Brubaker, J. Fowler, J. Hinnebusch, M. Marceau, C. Medigue, M. Simonet, V. Chenal-Francisque, B. Souza, D. Dacheux, J. M. Elliott, A. Derbise, L. J. Hauser, and E. Garcia.** 2004. Insights into the evolution of Yersinia pestis through whole-genome comparison with Yersinia pseudotuberculosis. Proc. Natl. Acad. Sci. USA **101:**13826–13831.

8. **Coburn, G. A., and G. A. Mackie.** 1999. Degradation of mRNA in *Escherichia coli*: an old problem with some new twists. Prog. Nucleic Acid Res. Mol. Biol. **62:**55–108.
9. **De Gregorio, E., C. Abrescia, M. S. Carlomagno, and P. P. Di Nocera.** 2002. The abundant class of *nemis* repeats provides RNA substrates for ribonuclease III in Neisseriae. Biochim. Biophys. Acta **1576:**39–44.
10. **De Gregorio, E., C. Abrescia, M. S. Carlomagno, and P. P. Di Nocera.** 2003. Asymmetrical distribution of *Neisseria* miniature insertion sequence DNA repeats among pathogenic and nonpathogenic *Neisseria* strains. Infect. Immun. **71:**4217–4221.
11. **De Gregorio, E., C. Abrescia, M. S. Carlomagno, and P. P. Di Nocera.** 2003. Ribonuclease III-mediated processing of specific Neisseria meningitidis mRNAs. Biochem. J. **374:**799–805.
12. **Deng, W., V. Burland, G. Plunkett III, A. Boutin, G. F. Mayhew, P. Liss, N. T. Perna, D. J. Rose, B. Mau, S. Zhou, D. C. Schwartz, J. D. Fetherston, L. E. Lindler, R. R. Brubaker, G. V. Plano, S. C. Straley, K. A. McDonough, M. L. Nilles. J. S. Matson, F. R. Blattner, and R. D. Perry.** 2002. Genome sequence of *Yersinia pestis* KIM. J. Bacteriol. **184:**4601–4611.
13. **Ehretsmann, C. P., A. J. Carpousis, and H. M. Krisch.** 1992. Specificity of Escherichia coli endoribonuclease RNase E: *in vivo* and *in vitro* analysis of mutants in a bacteriophage T4 mRNA processing site. Genes Dev. **6:**149–159.
14. **Feschotte, C., N. Jiang, and S. R. Wessler.** 2002. Plant transposable elements: where genetics meets genomics. Nat. Rev. Genet. **3:**329–341.
15. **Feschotte, C., L. Swamy, and S. R. Wessler.** 2003. Genome-wide analysis of mariner-like transposable elements in rice reveals complex relationships with stowaway miniature inverted repeat transposable elements (MITEs). Genetics **163:**747–758.
16. **Higgins, C. F., R. S. McLaren, and S. F. Newbury.** 1988. Repetitive extragenic palindromic sequences, mRNA stability and gene expression: evolution by gene conversion? A review. Gene **72:**3–14.
17. **Hulton, C. S. J., C. F. Higgins, and P. M. Sharp.** 1991. ERIC sequences, a novel family of repetitive elements in the genomes of *Escherichia coli*, *Salmonella typhimurium* and other enterobacteria. Mol. Microbiol. **5:**825–834.
18. **Jiang, N., C. Feschotte, X. Zhang, and S. R. Wessler.** 2004. Using rice to understand the origin and amplification of miniature inverted repeat transposable elements (MITEs). Curr. Opin. Plant Biol. **7:**115–119.
19. **Kaberdin, V. R.** 2003. Probing the substrate specificity of Escherichia coli RNase E using a novel oligonucleotide-based assay. Nucleic Acids Res. **31:**4710–4716.
20. **Kidwell, M. G., and D. R. Lisch.** 2000. Transposable elements and host genome evolution. Trends Ecol. Evol. **15:**95–99.
21. **Lin-Chao, S., T. T. Wong, K. J. McDowall, and S. N. Cohen.** 1994. Effects of nucleotide sequence on the specificity of *rne*-dependent and RNase E-mediated cleavages of RNA I encoded by the pBR322 plasmid. J. Biol. Chem. **269:**10797–10803.
22. **Liu, S. V., N. J. Saunders, A. Jeffries, and R. F. Rest.** 2002. Genome analysis and strain comparison of Correia repeats and Correia repeat-enclosed elements in pathogenic *Neisseria*. J. Bacteriol. **184:**6163–6173.
23. **Lopez, P. J., I. Marchand, O. Yarchuk, and M. Dreyfus.** 1998. Translation inhibitors stabilize Escherichia coli mRNAs independently of ribosome protection. Proc. Natl. Acad. Sci. USA **95:**6067–6072.
24. **Mazzone, M., E. De Gregorio, A. Lavitola, C. Pagliarulo, P. Alifano, and P. P. Di Nocera.** 2001. Whole-genome organization and functional properties of miniature DNA insertion sequences conserved in pathogenic Neisseriae. Gene **278:**211–222.
25. **McCarthy, J. E., B. Gerstel, B. Surin, U. Wiedemann, and P. Ziemke.** 1991. Differential gene expression from the Escherichia coli atp operon mediated by segmental differences in mRNA stability. Mol. Microbiol. **10:**2447–2458.
26. **McDowall, K. J., S. Lin-Chao, and S. N. Cohen.** 1994. A+U content rather than a particular nucleotide order determines the specificity of RNase E cleavage. J. Biol. Chem. **269:**10790–10796.
27. **Meyer, B. J., and J. L. Schottel.** 1992. Characterization of cat messenger RNA decay suggests that turnover occurs by endonucleolytic cleavage in a 3′ to 5′ direction. Mol. Microbiol. **9:**1095–1104.
28. **Meyer, B. J., A. E. Bartman, and J. L. Schottel.** 1996. Isolation of a mRNA instability sequence that is cis-dominant to the ompA stability determinant in Escherichia coli. Gene **179:**263–270.
29. **Oggioni, M. R., and J. P. Claverys.** 1999. Repeated extragenic sequences in prokaryotic genomes: a proposal for the origin and dynamics of the RUP element in Streptococcus pneumoniae. Microbiology **145:**2647–2653.
30. **Parkhill, J., B. W. Wren, N. R. Thomson, R. W. Titball, M. T. Holden, M. B. Prentice, M. Sebaihia, K. D. James, C. Churcher, K. L. Mungall, S. Baker, D. Basham, S. D. Bentley, K. Brooks, A. M. Cerdeno-Tarraga, T. Chillingworth, A. Cronin, R. M. Davies, P. Davis, G. Dougan, T. Feltwell, N. Hamlin, S. Holroyd, K. Jagels, A. V. Karlyshev, S. Leather, S. Moule, P. C. Oyston, M. Quail, K. Rutherford, M. Simmonds, J. Skelton, K. Stevens, S. Whitehead, and B. G. Barrell.** 2001. Genome sequence of Yersinia pestis, the causative agent of plague. Nature **413:**523–527.
31. **Plasterk, R. H., Z. Izsvak, and Z. Ivics.** 1999. Resident aliens: the Tc1/mariner superfamily of transposable elements. Trends Genet. **15:**326–332.
32. **Py, B., C. F. Higgins, H. M. Krisch, and A. J. Carpousis.** 1996. A DEAD-box RNA helicase in the Escherichia coli RNA degradosome. Nature **38:**169–172.
33. **Rakin, A., C. Noelting, S. Schubert, and J. Heesemann.** 1999. Common and specific characteristics of the high-pathogenicity island of *Yersinia enterocolitica*. Infect. Immun. **67:**5265–5274.
34. **Redder, P., Q. She, and R. A. Garrett.** 2001. Non-autonomous mobile elements in the crenarchaeon Sulfolobus solfataricus. J. Mol. Biol. **306:**1–6.
35. **Rychlik, W., and R. E. Rhoads.** 1989. A computer program for choosing optimal oligonucleotides for filter hybridization, sequencing and in vitro amplification of DNA. Nucleic Acids Res. **17:**8543–8551.
36. **Shao, H., and Z. Tu.** 2001. Expanding the diversity of the IS630-Tc1-mariner superfamily: discovery of a unique DD37E transposon and reclassification of the DD37D and DD39D transposons. Genetics **159:**1103–1115.
37. **Sharp, P. M.** 1997. Insertions within ERIC sequences. Mol. Microbiol. **24:**1314–1315.
38. **Sharples, G. J., and R. G. Lloyd.** 1990. A novel repeated DNA sequence located in the intergenic regions of bacterial chromosome. Nucleic Acids Res. **18:**6503–6508.
39. **Sousa, S., I. Marchand, and M. Dreyfus.** 2001. Autoregulation allows Escherichia coli RNase E to adjust continuously its synthesis to that of its substrates. Mol. Microbiol. **42:**867–878.
40. **Steitz, J. A.** 1969. Polypeptide chain initiation: nucleotide sequences of the three ribosomal binding sites in bacteriophage R17 RNA. Nature **224:**957–964.
41. **Thompson, J. D., D. G. Higgins, and T. J. Gibson.** 1994. CLUSTAL W: improving the sensitivity of progressive multiple sequence alignment through sequence weighting, position-specific gap penalties and weight matrix choice. Nucleic Acids Res. **22:**4673–4680.
42. **Trulzsch, K., A. Roggenkamp, C. Pelludat, A. Rakin, C. Jacobi, and J. Heesemann.** 2001. Cloning and characterization of the gene encoding periplasmic 2′,3′-cyclic phosphodiesterase of *Yersinia enterocolitica* O:8. Microbiology **147:**203–213.
43. **Versalovic, J., T. Koeuth, and J. R. Lupski.** 1991. Distribution of repetitive DNA sequences in eubacteria and application to fingerprinting of bacterial genomes. Nucleic Acids Res. **19:**6823–6831.
44. **Wren, B. W.** 2003. The yersiniae—a model genus to study the rapid evolution of bacterial pathogens. Nat. Rev. Microbiol. **1:**55–64.
45. **Zuker, M.** 1989. On finding all suboptimal foldings of an RNA molecule. Science **244:**48–52.